

## Reviewing the latest results from the Pierre Auger Observatory

---

**Carola Dobrigkeit\* for the Pierre Auger Collaboration<sup>†</sup>**

*Instituto de Física Gleb Wataghin, Universidade Estadual de Campinas, Campinas, SP, Brazil*

*E-mail: [carola@ifi.unicamp.br](mailto:carola@ifi.unicamp.br)*

*Full author list: [http://www.auger.org/archive/authors\\_2015\\_05.html](http://www.auger.org/archive/authors_2015_05.html)*

We report on the latest results from the Pierre Auger Observatory in its continuing mission of studying cosmic rays in the highest-energy region observed to date. Operating now for more than ten years, the data collected with the Auger Observatory have already led to major breakthroughs in our knowledge about these very rare particles. We mention specifically some recent results of data analyses performed involving their energy spectrum, mass composition, arrival direction distributions, and searches for neutral messengers like neutrinos, photons, and neutrons. Finally, in the light of the latest findings, we discuss the plans for the next challenges to be faced by the Collaboration with the goal of unraveling the main features of cosmic rays in the energy region of the flux suppression.

*XI Multifrequency Behaviour of High Energy Cosmic Sources Workshop*

*25-30 May 2015*

*Palermo, Italy*

---

\*Speaker.

<sup>†</sup>Observatorio Pierre Auger, Av. San Martín Norte, 304, 5613 Malargüe, Argentina

## 1. Introduction

Even though discovered a century ago, studying cosmic rays over the vast energy range they span still represents a challenge. The energy spectrum of cosmic particles reaching Earth covers nearly twelve decades in energy, and correspondingly thirty-two decades in flux. There are not many phenomena in physics that cover such a wide range in energy, from  $10^9$  eV to  $10^{20}$  eV. These particles stem from different origins, having passed through different production and acceleration processes, and traversed different environments to reach us. Here we will focus on the most energetic particles, those with energies from  $10^{17}$  eV to in excess of  $10^{20}$  eV.

Only three years after the observation of the first ultra-high energy cosmic ray (UHECR) by Linsley in 1963 [1], Greisen [2] and, independently, Zatsepin and Kuz'min [3] realised that such energetic bullets would be hindered in their propagation by interactions with photons from the then recently discovered cosmic microwave background radiation (CMBR). Following the predictions of these authors, if the particles were protons, they would lose energy producing pions through the delta resonance in  $p + \gamma_{2.7K} \rightarrow p + \pi^0$  or  $n + \pi^+$ . If they were heavier nuclei, they would suffer disintegration in  $A + \gamma_{R,2.7K} \rightarrow (A - 1) + n$ . Both photopion production and photodisintegration would result in their energy losses, potentially causing a flux suppression at energies around a few times  $10^{19}$  eV, or even a termination of the spectrum at some high-energy limit. This so-called GZK effect would also set a limit for the distance of potential cosmic-ray sources from Earth at maximally 200 Mpc.

Detecting UHECRs certainly presents considerable difficulties. The higher their energy, the rarer they get, and therefore a large area of detectors and a long observation time to collect a sample of the most energetic ones becomes necessary. Additionally, these particles are not directly observable. After entering the atmosphere they interact with nuclei in the atmosphere giving rise to a huge shower of secondary particles which eventually reach the ground, and are recorded. The signals left in the detectors permit the reconstruction of the shower geometry and of the energy of the primary cosmic ray that initiated the shower, as well as an estimation of the composition of these primaries.

The Pierre Auger Observatory is the largest cosmic-ray facility to date constructed with the goal of studying exactly these most energetic particles in the energy region from  $10^{17}$  eV to in excess of  $10^{20}$  eV, and finding clues about their origin and composition. The construction of the Observatory in its original conception ended in 2008, and various detectors have been incorporated in the past few years contributing to an increase in its detection capabilities. Here we address the latest results obtained with the Pierre Auger Observatory from data collected through ten years of uninterrupted operation, corresponding to an exposure of more than  $50\,000 \text{ km}^2 \text{ sr yr}$ .

## 2. The Pierre Auger Observatory

The Pierre Auger Observatory was the first cosmic-ray detector array to employ two complementary detection techniques aiming at a better accuracy in the measurements. A total of 1600 water-Cherenkov detector stations deployed on a triangular grid of 1500 m side and covering an area of  $3000 \text{ km}^2$  constitute the surface detector array (SD). With the SD the lateral distribution of particle densities at the ground is obtained. Four sites on the perimeter of the SD house six

air-fluorescence telescopes (FD) overlooking the atmosphere above the SD, and measuring the longitudinal development of air showers along their path down to the ground. While the telescopes require clear moon-less nights to operate, which represents  $\sim 13\text{--}15\%$  of the time, the surface detectors have a duty cycle of nearly 100%. Showers measured simultaneously with both the FD and the SD, the so-called hybrid showers, are used for energy calibration. To this aim, certain shower-characteristic quantities measured with the SD are related to the almost calorimetric energy measured with the FD, and a cross-calibration of the energy scale is obtained. The energy calibration is then extended to the full set of showers measured only with the SD. The detectors of the Auger Observatory as well as all calibration procedures are extensively described in [4].

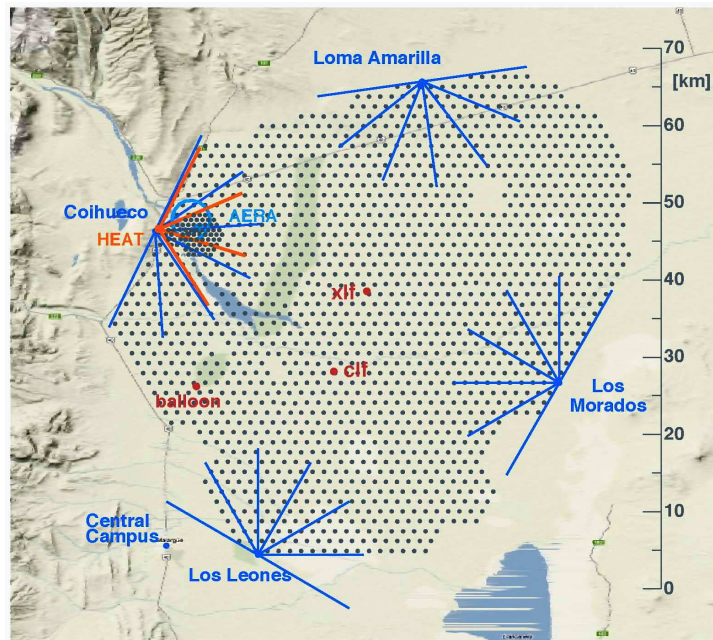


**Figure 1:** The Pierre Auger Observatory. Each dot corresponds to one of the surface detector stations. The four fluorescence detector sites are also depicted, with blue lines delimiting the  $30^\circ$  field of view of each of their six telescopes. Near the site of Coihueco at the west side, the locations of the denser surface-detector array, of the AERA radio-station array, and of the three high-elevation fluorescence telescopes HEAT (with orange lines delimiting their field of view) are shown, as well as the two laser facilities (CLF and XLF) near the center of the array, and the balloon-launching site used for atmospheric monitoring [5].

The Pierre Auger Observatory is situated near the town of Malargüe, in the province of Mendoza, Argentina, at 1400 m above sea level. The site is in a privileged location, on an almost flat terrain over the whole area with only some smooth hills from where the telescopes overlook the SD array. The atmosphere above the site is very clean, favouring measurements of the fluorescence light emitted by nitrogen molecules excited in the passage of the huge number of air-shower particles. The location of the Pierre Auger Observatory at coordinates  $32.5^\circ\text{S}$ ,  $69.5^\circ\text{W}$  further permits the observation of the region around the Galactic centre, which passes to within only a few degrees of its zenith.

Full detection efficiency is attained with the SD for showers with energies above  $3 \times 10^{18}$  eV (3 EeV) and zenith angles up to  $60^\circ$ . For more inclined showers with zenith angle between  $60^\circ$  and

$80^\circ$ , the array is fully efficient above  $4 \times 10^{18}$  eV. These two shower categories are dubbed *vertical* and *inclined* showers, respectively, following these classifications.

Since 2008, the detector capabilities of the Auger Observatory have been augmented over the years by adding new detectors and by exploring new detection techniques. Three tiltable High-Elevation Auger Telescopes (HEAT) allow the observation of fluorescence light originating from portions of the shower higher in the atmosphere. The Auger Engineering Radio Array (AERA) explores the potential of detecting air showers through the radio signal emitted while secondary particles propagate down the atmosphere. To this goal, 153 autonomous, dual-polarisation radio antennas are deployed over an area of  $17 \text{ km}^2$ , capturing the radio signals in the 30 to 80 MHz band. AERA offers the possibility of an independent energy assignment for each shower by profiting from a less expensive technique. By measuring the energy fraction transferred into radio pulses for each shower, it is possible to set an alternative estimator for the shower energy. Finally, an enhancement dedicated to the measurement of the muon content in air showers is under construction. The Auger Muon and Infilled Ground Array (AMIGA) is composed of a denser array of 60 surface stations nested in the SD, and deployed over  $23.5 \text{ km}^2$  at half the distance (750 m) of the regular array. In addition, scintillator detectors are buried nearby. We refer to the denser array as SD-750, to distinguish it from the regular array (SD-1500). This infilled array is located just in front of the Coihueco FD site, being overlooked by both regular and high-elevation telescopes, and permitting the measurement of showers with energies down to  $10^{17}$  eV. Full efficiency of the infilled array is attained for showers with energy above  $3 \times 10^{17}$  eV and zenith angles up to  $55^\circ$ .

The atmosphere above the Pierre Auger Observatory is extensively monitored during the periods of FD operations. To this aim, the Central Laser Facility (CLF) and the eXtreme Laser Facility (XLF) provide periodic measurements of the aerosol optical depths necessary for reconstruction of air showers measured with the FD. Until 2010, balloons were launched from the site to measure atmospheric profiles of state variables up to 20–25 km a.s.l. Since then, these data have been replaced by the accessible data from the Global Data Assimilation System (GDAS) after an appropriate validation. A detailed description of these facilities and their operation can also be found in [4].

In Fig. 1 a schematic layout of the Pierre Auger Observatory detector is shown, with each dot representing one of the 1660 surface detectors. Blue (orange) lines delimit the  $30^\circ$  field of view of the FD (HEAT) telescopes. The locations of AERA and of the two laser facilities are also depicted in the same figure [5].

### 3. Recent results

We present a selection of the latest results obtained by the Pierre Auger Observatory on the energy spectrum of the cosmic rays, on their mass composition, on analyses of arrival-direction distributions, and on searches for neutral cosmic messengers. These results provide hints about the origin and composition of UHECRs, as well as about potential sources or source regions in the portion of the sky covered by the observatory. Most of the results rely on air showers detected since 2004 over the last ten years. For the first time the analyses include also inclined showers, which require a dedicated procedure for their reconstruction [6]. The inclusion of inclined showers allows for an enlargement of 30% in the total exposure, simultaneously yielding a sky coverage of 85%

extending from  $-90^\circ$  to  $45^\circ$  in declination. Additionally, including inclined showers permits the setting of constraints on current models describing hadronic interactions at energies above those attainable with present accelerators.

### 3.1 Energy spectrum

In 2015, the Pierre Auger Collaboration reported the energy spectrum obtained from around 118 000 showers with the SD-1500 (15 000 of them inclined), 61 000 measured with the SD-750, and around 9 000 hybrid showers [7]. The spectrum obtained from these four data sets corresponds to an exposure exceeding  $50\,000\text{ km}^2\text{ sr yr}$ , and is shown in Fig. 2 (left). Systematic uncertainties in the flux are 5.8% (5%) for vertical (inclined) showers measured with the SD-1500 array. For the denser SD array, the corresponding value decreases from 14% at  $10^{17.5}\text{ eV}$  to 7% above  $10^{18.5}\text{ eV}$ . For hybrid showers, the uncertainties display the same tendency, diminishing from 10% at  $10^{18}\text{ eV}$  to less than 6% above  $10^{19}\text{ eV}$ .

Two features are clearly recognisable in the all-particle spectrum, and confirm earlier results reported by the Pierre Auger Collaboration. Considering that the overall tendency of the spectrum follows a power law  $E^{-\gamma}$  with energy, one easily identifies a hardening of the spectrum at  $E_{\text{ankle}} = (4.8 \pm 0.1 \pm 0.8) \times 10^{18}\text{ eV}$ , known as the "ankle", and a drastic flux suppression at the energy  $E_s = (42.1 \pm 1.7 \pm 7.6) \times 10^{18}\text{ eV}$ . Here  $E_s$  corresponds to the energy at which the *differential* flux reduces to one-half of the value expected from the extrapolation of the power-law behaviour observed at energies just above  $E_{\text{ankle}}$ . These values are obtained from the best fit of the all-particle spectrum shown in Fig. 2 (right), and all mentioned uncertainties refer to statistical and systematic ones, respectively. Below  $E_{\text{ankle}}$  the spectrum follows a power law with index  $\gamma = (-3.29 \pm 0.02 \pm 0.05)$ , while above that the index changes to  $\gamma = (-2.60 \pm 0.02 \pm 0.10)$ .

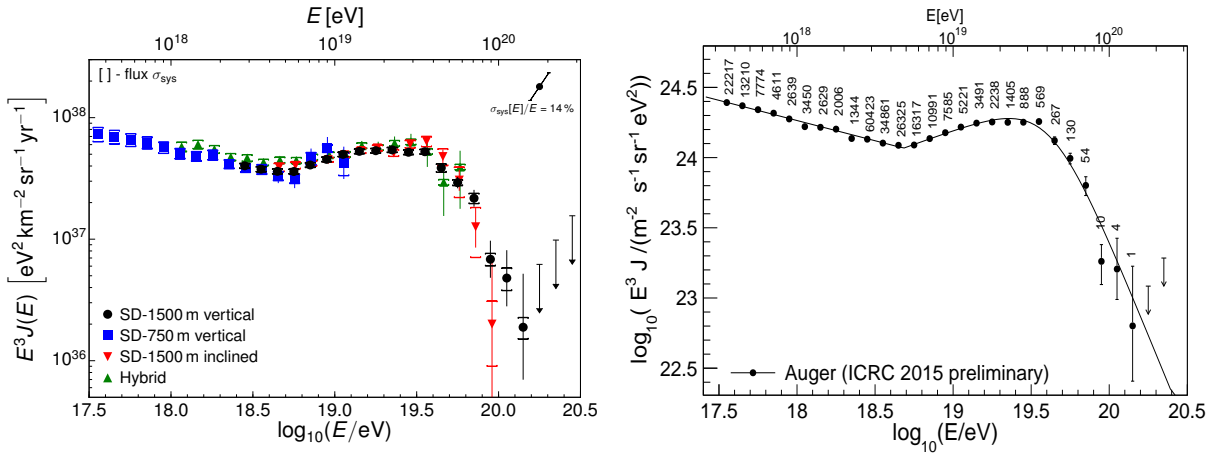


**Figure 2:** Left: the Auger energy spectrum obtained from hybrid showers, from SD data obtained with the 1500 m array for vertical and inclined showers, and from vertical showers with the infilled SD array. Right: The combined all-particle spectrum and corresponding fit, with the number of showers given in each  $\log E$  bin (right). The error bars represent only the statistical uncertainties. Upper limits correspond to the 84% confidence level [7].

The same data set of vertical showers obtained with the SD-1500 was also scrutinised looking for a potential dependence on declination. After correcting for experimental, atmospheric and

geomagnetic effects, the showers were separated into four declination bands with approximately equal exposures, and the corresponding spectra were obtained in each band. Fig. 3 (left) shows the resulting spectra [7]. No evidence of significant departures from the all-particle spectrum was observed, the agreement among them being within 5% below  $E_s$ , and within 14% above this energy.

The features of the ankle and flux suppression observed in the spectrum deserve special attention. The simplest interpretation of the ankle consists in associating it to the transition from a Galactic to an extragalactic cosmic-ray component at around  $10^{18}$  eV, with the first component gradually fading out, and the flux recovery at increasing energy being attributed to the extragalactic component taking over. This line of thought would result, for instance, from a mixed primary composition caused by the photonuclear disintegrations in interactions with the CMBR mentioned previously. As for the interpretation of the flux suppression, it could be simply described as being a manifestation of the GZK effect. Both the processes of photopion production and photodisintegration would then result in protons arriving at Earth.

But these are not the only possible interpretations of the two features. Alternatively, the so-called “dip model” [8] relies on the ankle reflecting pure extragalactic protons losing their energy via pair production processes. In this model the transition from the Galactic to the extragalactic component would occur at lower energies around  $10^{17}$  eV. As for the flux suppression, it can be described in a model scenario in which the sources inject protons with an energy spectrum following  $E^{-\beta}$  exponentially attenuated by a scale parameter  $E_{\text{cut}}$  of the order of  $10^{20}$  eV. Assuming a cosmological evolution of the source luminosity parameterised as  $(1+z)^m$ , and a continuous source distribution, a reasonably good description of the observed spectrum is obtained choosing  $m = 5$  and  $\beta = 2.35$ . This description was already presented as a possible interpretation in [9], comparing to the Auger spectrum at that time. It is shown in Fig. 3 (right) only as an illustration of the model, and to point out that the description of the observed spectrum demands cosmic rays to be protons. Therefore, both alternative interpretations mentioned here rely on UHECRs being protons. We are led to the conclusion that deciding among various scenarios requires knowing also the mass composition of the primary particles arriving at Earth, to cross-check whether these are protons or heavier nuclei. The mass composition will be addressed in the next section.

### 3.2 Mass composition

Unraveling the mass composition of ultra-high energy particles reaching Earth is challenging. For this goal, the Pierre Auger Collaboration studies the longitudinal development of air showers in the atmosphere, since it depends directly on the mass of the primary particle initiating it. Heavier primaries interact higher in the atmosphere than protons, and show smaller fluctuations in their development. The Pierre Auger Observatory measures the longitudinal shower profiles, allowing one to obtain both the atmospheric depth at which the number of shower particles attains its maximum, or in short, the slant depth of shower maximum  $X_{\text{max}}$ , and the fluctuations of this quantity,  $\sigma(X_{\text{max}})$ . Since these measurements rely on fluorescence observations, they suffer from the shorter duty cycle of the telescopes, and consequently of the decreasing number of showers with energy, especially in the highest energy region. The FD measures the longitudinal development of the shower in the atmosphere, and therefore is sensitive to the first interactions which occur near the top of the atmosphere. On the other hand, the SD registers the particles reaching the ground, and is therefore sensitive to the whole hadronic cascade.

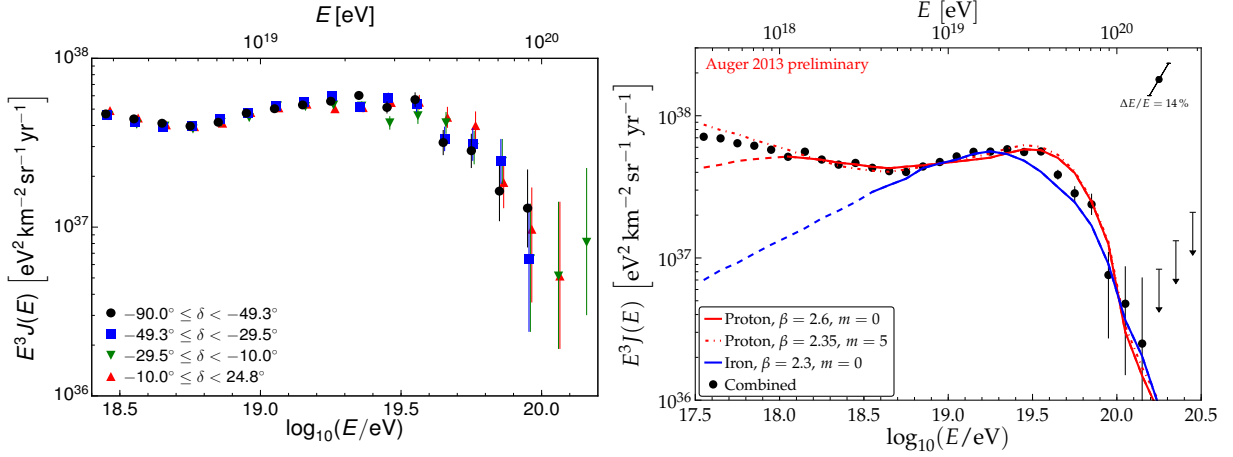


**Figure 3:** Left: Energy spectrum obtained from vertical showers measured with the SD in four declination bands [7]. Right: The combined Auger energy spectrum as of 2013, which at the time was compared to spectra obtained from different astrophysical scenarios [9], shown here only for illustration purposes.

The Auger Collaboration reported results of a thorough analysis of  $X_{\text{max}}$  distributions obtained from a nearly unbiased measurement of air showers with energies above  $10^{17.8}$  eV collected between December 2004 and December 2012 [10]. The first two moments of the distribution of  $X_{\text{max}}$  are compared to results from Monte Carlo simulations of complete air showers using the hadronic interaction models Sibyll 2.1 [11], QGSJetII-04 [12] and EPOS-LHC [13]. The last two models already have their parameters tuned to the most recent data from accelerator experiments at the LHC. In Fig. 4 the energy evolution of those two moments,  $\langle X_{\text{max}} \rangle$  and  $\sigma(X_{\text{max}})$  is presented. Assuming that the hadronic interaction models correctly describe the physical processes at energies of the relevant air showers, we infer a composition which is predominantly light between  $10^{18}$  eV and  $10^{18.5}$  eV, with the fraction of heavy nuclei increasing up to the highest energy around  $10^{19.6}$  eV. The mean of  $X_{\text{max}}$  and its dispersion were also converted to the first two moments of the corresponding  $\ln A$  distribution, revealing further details of the potential mass composition and interaction models. The evolution of the average composition towards light nuclei up to energies of  $10^{18.3}$  eV was confirmed, and also the gradual increase of  $\langle \ln A \rangle$  at increasing energy. It is interesting to mention that EPOS-LHC leads to the heaviest composition on average that is compatible with the  $\ln A$  of nitrogen nuclei at the highest energies. From the variance of  $\ln A$  derived from EPOS-LHC and Sibyll 2.1 one can infer that the flux of primary cosmic rays at low energies is composed of different nuclei, while at the higher energies it is dominated by a single species of nucleus, since the variance tends to zero. It can also be mentioned that the variance of  $\ln A$  obtained with QGSJetII-04 ends up negative, rendering unphysical values.

The same distributions presented in [10] were also used in an accompanying paper exploring the implications of these distributions both for the cosmic-ray composition and for hadronic interaction models [14]. To this aim, the  $X_{\text{max}}$  distributions were fitted to predictions from simulations of air showers initiated by different primary particles, using the same hadronic interaction models mentioned above. The observed  $X_{\text{max}}$  distributions cannot be described either assuming primary cosmic rays to be largely dominated by protons, or else largely dominated by iron nuclei. Inde-

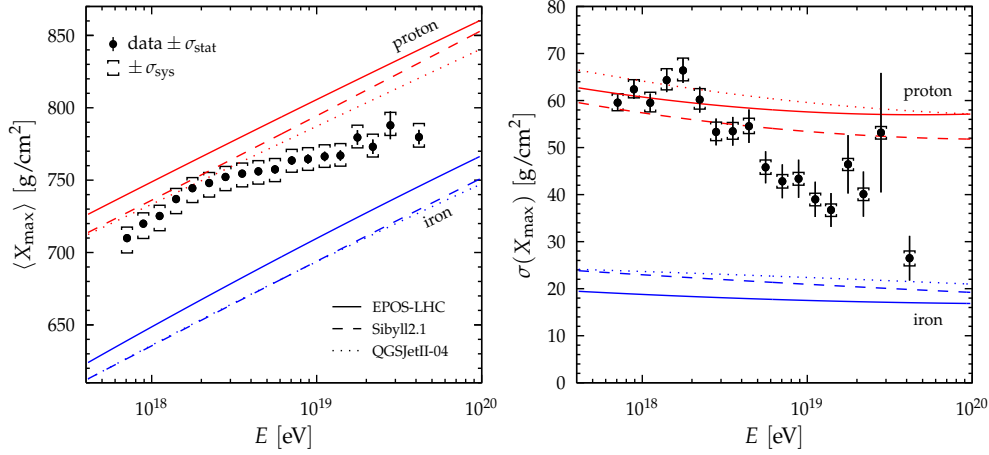


**Figure 4:** Energy evolution of the first two moments of the  $X_{\max}$  distribution, compared with predictions from simulations of air showers initiated by protons or iron nuclei [10].

pendently of the interaction model adopted in the simulations, it is found that a mixed composition of only protons and iron nuclei does not describe the observed distributions either, over most of the energy interval. On the other hand, acceptable descriptions of the distributions are obtained with the three models when the composition is supposed to include also intermediate nuclei, like helium and/or nitrogen, besides protons and iron nuclei. In particular, the proton fractions obtained from fits with all these models are consistent among themselves, and show the same evolution with energy. The fractions of the other three components differ from model to model. Additionally, none of the three models supports a significant contribution of iron nuclei in the primary flux. The resulting fractions obtained in the fits when assuming the four components protons, helium nuclei, nitrogen nuclei, and iron nuclei are shown in Fig. 5 with the corresponding  $p$ -values, and support the findings mentioned above.

### 3.3 Neutral cosmic messengers

Ultra-high energy neutrinos and photons are expected to be created either as secondaries of interactions of UHECRs in their source environment or during their propagation, or otherwise in the decay of heavy primordial particles in so-called top-down models. The Pierre Auger Observatory has the capability of detecting ultra-high energy neutrinos and photons with energies above 1 EeV and 10 EeV, respectively. The Auger SD can detect downward-going neutrinos of all flavours at zenith angles above  $60^\circ$  interacting in the atmosphere, and upward-going earth-skimming tau neutrinos, as well as photons with zenith angles between  $30^\circ$  and  $60^\circ$  [15]. The criteria for selecting showers initiated by these particles can be found in [15] and references therein.

After applying the selection criteria to the data, no shower collected between 01 January 2004 and 20 June 2013 is selected with the neutrino cuts [16], while four showers survive the photon cuts in the period between 01 January 2004 and 15 May 2013.

Stringent limits are set to the diffuse fluxes of ultra-high energy neutrinos and photons, assuming a differential flux following a dependency  $dN(E) = k \cdot E^{-2}$ . The corresponding exposures are then estimated by applying the same selection criteria to simulated showers induced by primary



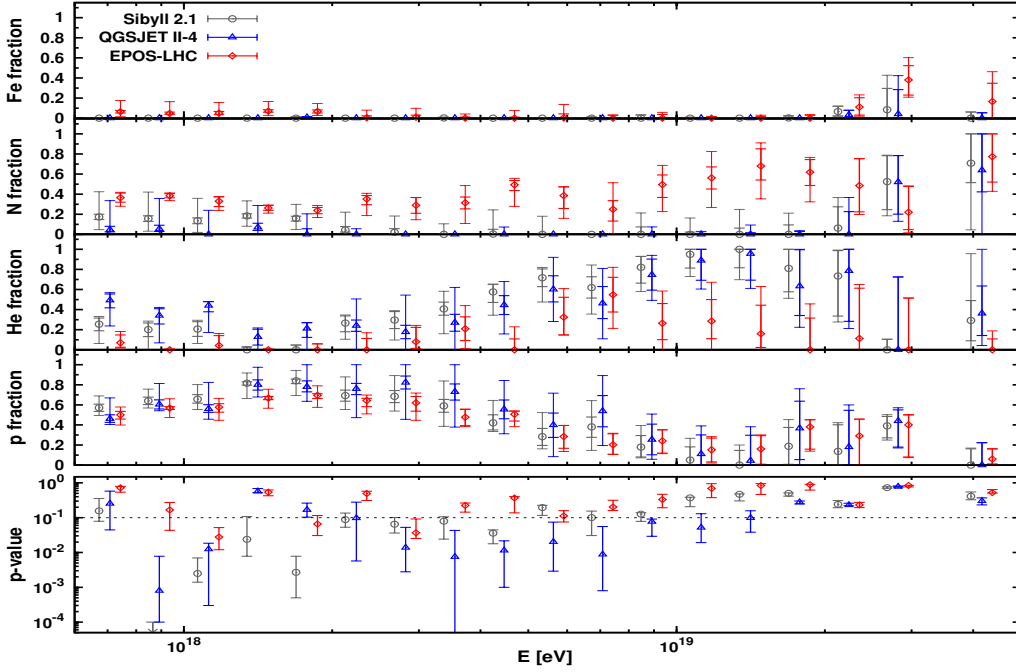


**Figure 5:** Fitted fractions obtained with the three interaction models when assuming a mixture of protons, helium nuclei, nitrogen nuclei, and iron nuclei, with corresponding  $p$ -values [14].

neutrinos and hadrons.

In Fig. 6, upper limits of the diffuse flux of ultra-high neutrinos at the 90% confidence level are shown in integrated form (horizontal lines). The limit described in [15] (red line) is compared with predictions from cosmogenic models [17] [18] [19] [20], with the Waxman-Bahcall bound [21], and with limits from the IceCube [22] and ANITA experiments [23]. In this figure all neutrino fluxes are estimated for a single flavour. It is worth mentioning that the Auger limit falls below the Waxman-Bahcall limit, which is considered a theoretical benchmark.

The Pierre Auger Observatory is also sensitive to photon-induced showers, which are distinguishable from hadronic showers since they develop deeper in the atmosphere, corresponding to a larger depth of shower maximum, and since they comprise a lower harvest of muons at the ground. Therefore, it is possible to search for primary photons by selecting the characteristic time structure of the photon signals in the SD stations, associated with the particular shapes of the lateral distribution of these showers. The selection procedure is described in detail in [15]. Applying these criteria leaves four candidates in the event set from 01 January 2004 until 15 May 2013, compatible with the background from hadronic showers. The corresponding exposure is obtained by applying the same criteria to simulated showers induced by primary photons and hadrons, and assuming the same differential spectrum as for neutrinos, namely  $dN(E) = k.E^{-2}$ . Finally, the upper limit to the diffuse photon flux can be estimated at the 95% confidence level, as depicted in Fig. 7. Also shown in this same figure are previous results from the Pierre Auger Observatory (Hyb and SD 2008), marked in blue and gray arrows [24], together with results from Telescope Array (TA) [25], Yakutsk (Y) [26], Haverah Park (HP) [27], AGASA (A) [28], as well as with predictions from

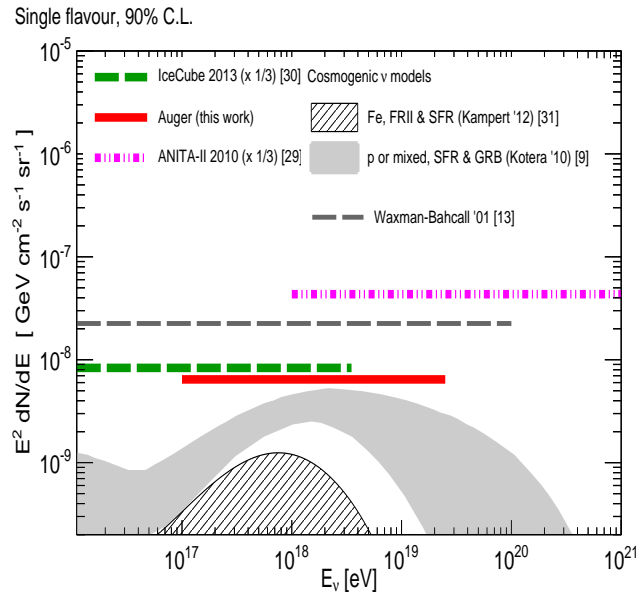


**Figure 6:** Upper limits to the diffuse flux of UHE neutrinos at the 90% confidence level, in integrated form (horizontal red line). The limit described in [15] (red line) is compared to those predicted from cosmogenic neutrino models [17] [18] [19] [20], to the Waxman-Bahcall bound [21], and to limits from IceCube [22] and ANITA experiments [23].

top-down models [29] [30] and cosmogenic photon models [18] [19] [29]. The Auger flux limits clearly disfavour top-down models of photon production.

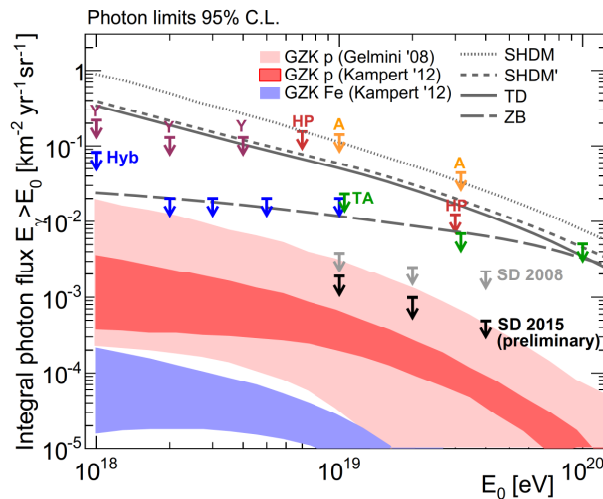


**Figure 7:** Upper limits of the diffuse flux of ultra-high energy photons at the 95% confidence level, marked in black arrows as SD 2015. Previous Auger results (Hyb and SD 2008) are marked in blue and gray arrows [24]. Also shown are results from Telescope Array (TA), Yakutsk (Y), Haverah Park (HP), AGASA (A), as well as predictions from top-down models, and cosmogenic photon models [15]. For the detailed references, see text.

If there exist Galactic sources emitting ultra-high energy neutrons, these would be detectable

by the Pierre Auger Observatory if they lie in its field of view. Due to relativistic time dilation, the decay length of such neutrons would amount to  $9.2(E/\text{EeV})$  kpc. If their energy is above 4 EeV, they would even be able to cross our entire Galaxy.

Neutron-induced showers are indistinguishable from those initiated by protons. Nevertheless, being electrically neutral, neutrons are not deflected in the intervening magnetic fields during their propagation. Therefore, if detected, they would point directly to their source. The Pierre Auger Collaboration has performed a search for such neutron showers, looking for flux excesses in small angular windows in the sky in its field of view. No statistically significant excess was detected [31]. The Auger data were also scrutinised in a stacked analysis of candidate Galactic sources of neutrons, with the same outcome [32]. The limits that can be set on the neutron flux constrain models of non-transient EeV proton sources in our Galaxy.

### 3.4 Anisotropy studies

The Pierre Auger Collaboration has performed various analyses of the arrival direction distributions motivated by the search for sources or source regions of UHECRs in the sky. Recently, the Collaboration reported results of studies over both large and small angular scales. Here we will address solely the large-scale studies, since there is another presentation at this workshop fully dedicated to the small-scale searches [33].

The latest analysis of arrival direction distributions over large angular scales already profits from the inclusion of inclined showers in the data set, and involves 70 000 showers with energies above 4 EeV, at full detection efficiency for both vertical and inclined showers [34]. In this work atmospheric and geomagnetic effects are accounted for, as well as the partial sky exposure. The influence of the small tilt of the surface array over the horizontal plane as small as  $0.2^\circ$  is also taken into consideration, and so is also the effect of the varying array area during the construction period.

Rayleigh analyses are performed both in right ascension and in azimuthal angle, and the dipole components are obtained along the equatorial plane and along the Earth's rotation axis. The data are divided into two sets corresponding to the energy bands  $4 \text{ EeV} < E < 8 \text{ EeV}$  and  $E > 8 \text{ EeV}$ . Assuming that only the dipole components contribute significantly leads to resulting dipole components of  $\approx 3\%$  and  $\approx 7\%$  in the two energy bands respectively, with only the latter being significant. No significant departure from isotropy is observed in the distributions of arrival directions of the lower-energy particles. The quadrupole components turn out compatible with zero in both energy intervals.

In the energy band  $E > 8 \text{ EeV}$  a dipole results, with amplitude  $(0.073 \pm 0.015)$  and pointing in the direction  $(\alpha, \delta) = (95^\circ \pm 13^\circ, -39^\circ \pm 13^\circ)$ . The sky map of the cosmic-ray flux is presented in Fig. 8 (left) after applying a smoothing in angular windows of  $45^\circ$  [35].

The possibility of a combination of a dipole and a quadrupole is also considered in the analysis, and confirmed that only the dipole term is significant, although with lower significance than when considered to be the only term contributing. A possible interpretation of the dipole term is a potential inhomogeneity in the distribution of nearby sources. An alternative to explain a dipolar anisotropy of a few percent above 8 EeV would be the diffusive propagation of extragalactic cosmic rays in turbulent magnetic fields, as shown for instance in [37]. This could result either if the amplitude of the field is large or if the cosmic rays are heavy and have a large electric charge.

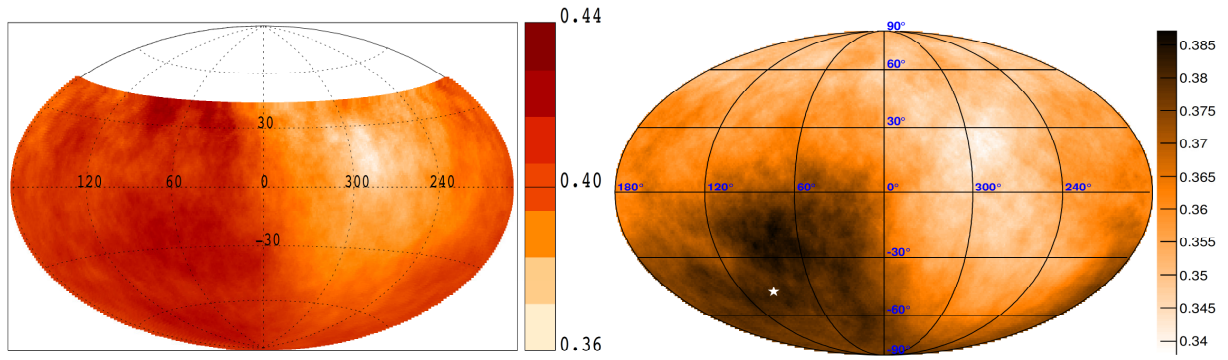


**Figure 8:** Left: Sky map of the cosmic-ray flux above 8 EeV with a smoothing in angular windows of  $45^\circ$  [35]. Right: Sky map of the full-sky cosmic flux above 10 EeV using data from both Auger and TA, with a smoothing in angular windows of  $60^\circ$ . The direction of the reconstructed dipole is represented by the white star [36]. Both fluxes are shown in equatorial coordinates, and the color scales represent the fluxes in units of  $\text{km}^{-2} \text{sr}^{-1} \text{yr}^{-1}$ .

An interesting study also over large angular scales was recently presented by the Pierre Auger Collaboration and the Telescope Array Collaboration (TA). The TA Observatory is located in the Northern hemisphere, at a latitude of  $39.3^\circ$  N. Merging the data sets of the two collaborations renders full sky coverage, therefore exempting the analysis from any previous assumption about the flux [36], [39]. The study included 17 000 showers from the Pierre Auger Observatory and another 2 500 ones from TA. The total flux is depicted in Fig. 8 (right) with a smoothing in angular windows of  $60^\circ$ . The joint analysis resulted in a dipole amplitude of  $(0.065 \pm 0.019)$  for cosmic rays with energies  $E > 10$  EeV pointing in the direction  $(\alpha, \delta) = (93^\circ \pm 24^\circ, -46^\circ \pm 18^\circ)$ , as marked with the white star in the figure. The probability of obtaining this amplitude by chance from an isotropic distribution amounts to  $5 \times 10^{-3}$ . The dipole was the only term in the analysis deviating from fluctuations of an isotropic flux distribution at the 99% confidence level.

Finally we report the results of a harmonic analysis performed on a set of cosmic rays over the energy region 0.02 up to 20 EeV, an important interval for studying the transition from Galactic to extragalactic cosmic rays. The harmonic analysis was performed on the right ascension of arrival directions. The amplitudes resulted at the level expected from isotropy at the 99% confidence level, but the phases of the first harmonic show a surprising evolution with energy. In the low-energy region below 1 EeV the phases point to the right ascension of the Galactic centre region, and as energy increases there is a gradual change so that the phases finally point in a direction close to the anti-Galactic centre at the highest energies [38]. Fig. 9 presents the results of this analysis, showing the amplitudes (left) and phases (right) as a function of energy. The continuous line shown in the right plot corresponds to the value of right ascension  $\varphi = 263^\circ$ , and together with the dashed line results from a fit reported in [39].

These interesting results led the Pierre Auger Collaboration to propose a prescribed test which is currently running. The prescribed exposure in the test is expected to be attained in the second half of 2015. An intermediate update of the prescription can be found in [35], although still preliminary since the final prescribed exposure has not been attained.

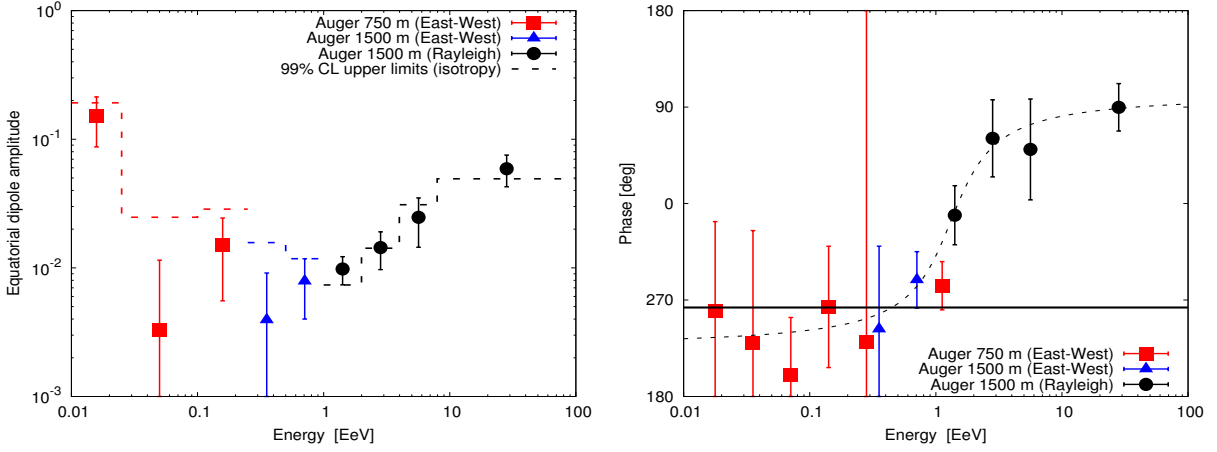


**Figure 9:** Equatorial dipole amplitude (left) and phase of the first harmonic in the arrival direction distribution (right) as a function of energy from data up to 2011 [38]. An intermediate update of these results can be found in [35], although still preliminary since the final prescribed exposure has not been attained yet.

#### 4. Conclusions and perspectives

The results obtained with the Pierre Auger Observatory in the analyses of data collected over the last ten years have been contributing to increase our knowledge about UHECRs. The ankle and the flux suppression observed in the energy spectrum are unequivocally confirmed. Nonetheless, the physical processes behind them cannot be completely certified at this time. The analysis of the longitudinal development of air showers up to the highest energies covered by the fluorescence telescopes reveals a surprising behaviour of  $X_{\max}$ . When interpreted in the light of our current knowledge, the behaviour seems to indicate a change from a mixed composition around  $10^{17}$  eV as shown in [40], to a light one in the interval  $10^{18}$  eV –  $10^{18.5}$  eV, and tending to a heavier one in the region at which the flux suppression is observed. Nevertheless, these interpretations about compositions rely on comparisons with the behaviour observed in simulated showers initiated by protons and iron nuclei. Although the hadronic interaction models adopted in shower simulations are already tuned to the most recent results from the LHC experiments, one should not forget that the centre-of-mass energies involved in UHECR collisions in the atmosphere can be one order of magnitude higher in energy. Some further inconsistencies are revealed when adopting the same LHC-tuned interaction models in the analysis of the muonic component of air shower, indicating a potential deficit in the muon production in simulations with respect to the one in observed showers. Additionally, recent studies of the muonic component seem to confirm the tendency to heavier primaries with increasing energy [41] [42] [43]. The observations of the longitudinal shower development and of the muonic component leave the possibility open for new properties of hadronic interactions to set in at energies beyond that in reach of LHC experiments. Therefore one cannot exclude the possibility that interactions of cosmic rays at energies as high as a few times  $10^{19}$  eV are not fully described when extrapolating models validated at lower energies. Another possible interpretation would be an unforeseen change in the properties of hadronic interactions at these extreme energies. Increasing the observed number of cosmic rays in the energy region of the flux suppression seems mandatory to successfully proceed.

Analyses of the arrival direction distribution of UHECRs have evidenced their high degree of isotropy, with the exceptions of an indication of a small dipole component at energies exceeding 8 EeV, and the surprising evolution of the phase of the first harmonic in approximately the same energy region. The largest deviations from an isotropic behaviour are observed for cosmic rays with energy above 58 EeV, in angular windows of  $\sim 20^\circ$  as reported in these proceedings [33], well in the region in which the flux suppression takes on.

From these results, the need of a better understanding of the mass composition of UHECRs stands out, and motivates the Pierre Auger Collaboration to concentrate major efforts in this direction. An upgrade of the Pierre Auger Observatory is presently proposed, with the main goal of providing additional measurements of composition-sensitive observables. The ultimate goal driving the upgrade efforts is to reach a better identification of the mass of the primary particles. To this end, the plan includes adding scintillator detectors on top of the existing surface detectors, so that the electromagnetic and muonic components are measured with two different detectors (SD and scintillators), and it becomes possible to disentangle them. In parallel, a modernisation of the by-now fifteen-year old electronics is foreseen, replacing the current systems with a three-times faster one, and incorporating new technological advances using modern microprocessors and FPGAs. More FD data in the highest-energy region will be procured by operating the telescopes under a higher night-sky background, thereby extending the duty cycle of the telescopes. Finally, the plans also include the continuation of deployment of the AMIGA muon detectors in the infilled area of the Observatory. All these actions aim to elucidate the mass composition so as to be able to fully interpret the cause of the flux suppression, allowing a clarification of whether the flux suppression is due to the GZK effect or signals a limit of the injection energy at the sources. Identifying the mass of the primary particles will also allow the selection of proton showers for studies of their arrival directions and of their longitudinal development in the atmosphere, providing a deeper understanding of hadronic interactions at the highest energies.

We are looking forward to extending the operation of the upgraded Observatory from 2018 until 2024, obtaining high-quality data and more than doubling the data set for our studies. Once the nature of the primary particles is better understood, the perspectives for future analyses become very promising, and conclusive interpretations of the results will be in reach.

## 5. Acknowledgements

The successful installation, commissioning, and operation of the Pierre Auger Observatory would not have been possible without the strong commitment and effort from the technical and administrative staff in Malargüe. The author acknowledges the financial support from the Fundação de Amparo à Pesquisa do Estado de São Paulo (FAPESP) through grant 2010/07359-6 and also from the Conselho Nacional de Desenvolvimento Científico e Tecnológico (CNPq) in Brazil.

## References

- [1] J. Linsley. *Evidence for a primary cosmic-ray particle with energy  $10^{20}$  eV*. Phys. Rev. Lett. **10**, 146 (1963).
- [2] K. Greisen. *End to the cosmic-ray spectrum?* Phys. Rev. Lett. **16**, 748 (1966).

- [3] G. T. Zatsepin and V. A. Kuz'min. *Upper limit of the cosmic ray spectrum*. JETPL **4**, 78 (1966).
- [4] A. Aab et al. (The Pierre Auger Collaboration). *The Pierre Auger Cosmic Ray Observatory*. Nucl. Instrum. Meth. A **798**, 172 (2015).
- [5] P. L. Ghia. *Highlights of the Pierre Auger Observatory*. To appear in Proc. of the 34th ICRC, The Hague, The Netherlands. PoS(ICRC2015) (2015).
- [6] A. Aab et al. (The Pierre Auger Collaboration). *Reconstruction of inclined air showers detected with the Pierre Auger Observatory*. JCAP **08**, 019 (2014).
- [7] I. Valiño for the Pierre Auger Collaboration. *The flux of ultra-high energy cosmic rays after ten years of operation of the Pierre Auger Observatory*. Proc. of the 34th ICRC, The Hague, The Netherlands. PoS(ICRC2015)271 (2015).  
[http://pos.sissa.it/archive/conferences/236/271/ICRC2015\\_271.pdf](http://pos.sissa.it/archive/conferences/236/271/ICRC2015_271.pdf)
- [8] V. Berezhinsky, G. Gazizov, S. Grigorieva. *On astrophysical solution to ultrahigh energy cosmic rays*. Phys. Rev. D **74**, 043005 (2006).
- [9] A. Schulz for the Pierre Auger Collaboration. *The measurement of the energy spectrum of cosmic rays above  $3 \times 10^{17}$  eV with the Pierre Auger Observatory*. Proc. of the 33rd ICRC, Rio de Janeiro, Brazil (2013). <http://www.cbpf.br/~icrc2013/papers/icrc2013-0769.pdf>
- [10] A. Aab et al. (The Pierre Auger Collaboration). *Depth of maximum of air-shower profiles at the Pierre Auger Observatory. I. Measurements at energies above  $10^{17.8}$  eV*. Phys. Rev. D **90**, 122005 (2014).
- [11] E.-J. Ahn et al. *Cosmic ray interaction event generator SIBYLL 2.1*. Phys. Rev. D **80** 094003 (2009).
- [12] S. Ostapchenko. *Non-linear screening effects in high energy hadronic interactions*. Phys. Rev. D **74**, 014026 (2006).
- [13] K. Werner et al. *Parton ladder splitting and the rapidity dependence of transverse momentum spectra in deuteron-gold collisions at RHIC*. Phys. Rev. C **74**, 044902 (2006).
- [14] A. Aab et al. (The Pierre Auger Collaboration). *Depths of Maximum of Air-Shower Profiles at the Pierre Auger Observatory: Composition Implications*. Phys. Rev. D **90**, 122006 (2014).
- [15] C. Bleve for the Pierre Auger Collaboration. *Updates on the neutrino and photon limits from the Pierre Auger Observatory*. Proc. of the 34th ICRC, The Hague, The Netherlands. PoS(ICRC2015)1103 (2015).  
[http://pos.sissa.it/archive/conferences/236/1103/ICRC2015\\_1103.pdf](http://pos.sissa.it/archive/conferences/236/1103/ICRC2015_1103.pdf)
- [16] A. Aab et al. (The Pierre Auger Collaboration). *An improved limit to the diffuse flux of ultra-high energy neutrinos from the Pierre Auger Observatory*. Phys. Rev. D **91**, 092008 (2015).
- [17] M. Ahlers et al. *GZK Neutrinos after the Fermi-LAT Diffuse Photon Flux Measurement*. Astropart. Phys. **34**, 106 (2010).
- [18] K.-H. Kampert, M. Unger. *Measurements of the Cosmic Ray Composition with Air Shower Experiments*. Astropart. Phys. **35**, 660 (2012).
- [19] B. Sarkar et al. *Ultra-High Energy Photon and Neutrino Fluxes in Realistic Astrophysical Scenarios*. Proc. 32nd ICRC Beijing, China, **2**, 198 (2011). <http://galprop.stanford.edu/eLibrary/icrc/2011/papers/HE1.3/icrc1087.pdf>
- [20] K. Kotera, D. Allard, A. V. Olinto. *Cosmogenic Neutrinos: parameter space and detectability from PeV to ZeV*. JCAP **10**, 013 (2010).

- [21] J. Bahcall, E. Waxman. *High energy astrophysical neutrinos: The upper bound is robust*. Phys. Rev. D **64**,023002 (2001).
- [22] M. G. Aartsen et al. (IceCube Collaboration). *Probing the origin of cosmic rays with extremely high energy neutrinos using the IceCube Observatory*. Phys. Rev. D **88**, 112008 (2013).
- [23] P. W. Gorham et al. (ANITA Collaboration). *Observational constraints on the ultrahigh energy cosmic neutrino flux from the second flight of the ANITA experiment*. Phys. Rev. D **85**, 049901(E) (2012).
- [24] P. Abreu et al. (The Pierre Auger Collaboration). *Upper limit on the cosmic-ray photon flux above  $10^{19}$  eV using the surface detector of the Pierre Auger Observatory*. Astropart. Phys. **29**, 243 (2008).
- [25] T. Abu-Zayyad et al. (Telescope Array Collaboration). *Upper limit on the flux of photons with energies above  $10^{19}$  eV using the Telescope Array surface detector*. Phys. Rev D **88**, 112005 (2013).
- [26] A. V. Glushkov et al. (Yakutsk EAS Array). *Constraints on the flux of primary cosmic-ray photons at energies  $E > 10^{18}$  eV from Yakutsk muon data*. Phys. Rev. D **82**, 041101 (2010).
- [27] M. Ave et al. *New Constraints from Haverah Park Data on the Photon and Iron Fluxes of Ultrahigh-Energy Cosmic Rays*. Phys. Rev. Lett. **85**, 2244 (2000).
- [28] K. Shinozaki et al. *Upper Limit on Gamma-Ray Flux above  $10^{19}$  eV Estimated by the Akeno Giant Air Shower Array Experiment*. ApJ **571**, L117 (2002).
- [29] G. Gelmini, O. Kalashev, D. Semikoz. *GZK photons as ultra-high-energy cosmic rays*. JETP **106**, 1061 (2008).
- [30] J. Ellis, V. E. Mayes, D. V. Nanopoulos. *Ultrahigh-energy cosmic rays particle spectra from crypton decays*. Phys. Rev. D **74**, 115003 (2006).
- [31] A. Aab et al. (The Pierre Auger Collaboration). *A Search for Point Sources of EeV Neutrons*. ApJ **760**, 149 (2012).
- [32] A. Aab et al. (The Pierre Auger Collaboration). *A Targeted Search for Point Sources of EeV Neutrons*. ApJ **789**, L34 (2014).
- [33] L. Caccianiga for the Pierre Auger Collaboration. *On ultra-high energy cosmic rays arrival directions after ten years of operation of the Pierre Auger Observatory*. These PoS Proceedings (2015).
- [34] A. Aab et al. (The Pierre Auger Collaboration). *Large scale distribution of ultra high energy cosmic rays detected at the Pierre Auger Observatory with zenith angles up to 80 degrees*. ApJ **804**, 15 (2015).
- [35] I. A. Samarai for the Pierre Auger Collaboration. *Indications of anisotropy at large angular scales in the arrival directions of cosmic rays detected at the Pierre Auger Observatory*. Proc. of the 34th ICRC, The Hague, The Netherlands. PoS(ICRC2015)372 (2015).  
[http://pos.sissa.it/archive/conferences/236/372/ICRC2015\\_372.pdf](http://pos.sissa.it/archive/conferences/236/372/ICRC2015_372.pdf)
- [36] O. Deligny for the Pierre Auger Collaboration. *Large-Scale Distribution of Arrival Directions of Cosmic Rays Detected at the Pierre Auger Observatory and the Telescope Array above  $10^{19}$  eV*. Proc. of the 34th ICRC, The Hague, The Netherlands. PoS(ICRC2015)375, (2015).  
[http://pos.sissa.it/archive/conferences/236/372/ICRC2015\\_375.pdf](http://pos.sissa.it/archive/conferences/236/372/ICRC2015_375.pdf)
- [37] D. Harari, S. Mollerach, E. Roulet. *Anisotropies of ultra-high energy cosmic ray nuclei diffusing from extragalactic sources*. Phys. Rev. D **92**, 063014 (2015).
- [38] I. Sidelnik for the Pierre Auger Collaboration. *Measurement of the first harmonic modulation in the right ascension distribution of cosmic rays detected at the Pierre Auger Observatory: towards the detection of dipolar anisotropies over a wide energy range*. Proc. of the 33rd ICRC 2013, Rio de Janeiro, Brazil (2013). <http://www.cbpf.br/~icrc2013/papers/icrc2013-0739.pdf>



- [39] P. Abreu et al. (The Pierre Auger Collaboration). *Search for first harmonic modulation in the right ascension distribution of cosmic rays detected at the Pierre Auger Observatory*. *Astropart. Phys.* **34**, 627 (2011).
- [40] A. Porcelli for the Pierre Auger Collaboration. *Measurements of  $X_{\max}$  above  $10^{17}$  eV with the fluorescence detector of the Pierre Auger Observatory*. Proc. of the 34th ICRC, The Hague, The Netherlands. PoS(ICRC2015)420 (2015).  
[http://pos.sissa.it/archive/conferences/236/420/ICRC2015\\_420.pdf](http://pos.sissa.it/archive/conferences/236/420/ICRC2015_420.pdf)
- [41] G. Farrar for the Pierre Auger Collaboration. *The muon content of hybrid events recorded at the Pierre Auger Observatory*. Proc. of the 33rd ICRC, Rio de Janeiro, Brazil (2013).  
<http://www.cbpf.br/~icrc2013/papers/icrc2013-1108.pdf>
- [42] A. Aab et al. (The Pierre Auger Collaboration). *Muons in air showers at the Pierre Auger Observatory: mean number in highly inclined events*. *Phys. Rev. D* **91**, 032003 (2015).
- [43] A. Aab et al. (The Pierre Auger Collaboration). *Muons in air showers at the Pierre Auger Observatory: measurement of atmospheric production depth*. *Phys. Rev. D* **90**, 012012 (2014).